



You have downloaded a document from
RE-BUŚ
repository of the **University of Silesia in Katowice**

Title: The Occurrence of Selected Radionuclides and Rare Earth Elements in Waste at the Mine Heap from the Polish Mining Group

Author: Danuta Smółka-Danielowska, Agata Walencik-Łata

Citation style: Smółka-Danielowska Danuta, Walencik-Łata Agata. (2021). The Occurrence of Selected Radionuclides and Rare Earth Elements in Waste at the Mine Heap from the Polish Mining Group. "Minerals" (2021), Vol. 11, art. no. 504. DOI: 10.3390/min11050504



Uznanie autorstwa - Licencja ta pozwala na kopiowanie, zmienianie, rozprowadzanie, przedstawianie i wykonywanie utworu jedynie pod warunkiem oznaczenia autorstwa.



UNIwersYTET ŚLĄSKI
W KATOWICACH




Biblioteka
Uniwersytetu Śląskiego



Ministerstwo Nauki
i Szkolnictwa Wyższego

Article

The Occurrence of Selected Radionuclides and Rare Earth Elements in Waste at the Mine Heap from the Polish Mining Group

Danuta Smolka-Danielowska ^{1,*}  and Agata Walencik-Łata ²

¹ Institute of Natural Sciences, Faculty of Natural Sciences, University of Silesia in Katowice, 41-200 Sosnowiec, Poland

² August Chełkowski Institute of Physics, University of Silesia in Katowice, 41-500 Chorzów, Poland; agata.walencik@us.edu.pl

* Correspondence: danuta.smolka-danielowska@us.edu.pl

Abstract: The paper presents the results of research on rare earth elements (REY) and selected radionuclides in barren rocks deposited on a heap at a mine belonging to the Polish Mining Group (the largest producer of hard coal in EU countries). The maximum concentration of REE_s determined in silstones was 261.6 mg/kg and in sandstones 221.2 mg/kg. The average uranium and thorium content in silstones was 6.8 mg/kg and 11.6 mg/kg, respectively. On the other hand, the samples of burnt coal shales contain on average 3.5 mg/kg of uranium and 9.7 mg/kg of thorium. In all coal waste samples, the REE values are higher than in hard coal (15.7 mg/kg). Carriers of REY, uranium, and thorium in coal waste are detritic minerals: monazite and xenotime, which are part of the grain skeleton of barren rocks. Coal waste samples are characterized by a variable distribution of REY concentrations as well as a variable content of radionuclides. The ²²⁶Ra, ²²⁸Ra, and ⁴⁰K measurements in the investigated samples were performed using the gamma spectrometry technique. The concentrations of the analyzed isotopes differed depending on the mineralogical composition of the investigated samples. The present study results may be important in determining the possibility of utilization of wastes of barren rocks stored in the mine heap and in assessing environmental and radiological hazards.

Keywords: coal waste; radionuclides; REE; mineral phases; environmental risk



Citation: Smolka-Danielowska, D.; Walencik-Łata, A. The Occurrence of Selected Radionuclides and Rare Earth Elements in Waste at the Mine Heap from the Polish Mining Group. *Minerals* **2021**, *11*, 504. <https://doi.org/10.3390/min11050504>

Academic Editors: Yasushi Watanabe, Shifeng Dai and Pierfranco Lattanzi

Received: 27 February 2021

Accepted: 6 May 2021

Published: 11 May 2021

Publisher's Note: MDPI stays neutral with regard to jurisdictional claims in published maps and institutional affiliations.



Copyright: © 2021 by the authors. Licensee MDPI, Basel, Switzerland. This article is an open access article distributed under the terms and conditions of the Creative Commons Attribution (CC BY) license (<https://creativecommons.org/licenses/by/4.0/>).

1. Introduction

Hard coal production is associated with the generation of significant amounts of mining waste, which amounts to about 34 million megagram (Mg) annually in Poland [1]. It is estimated that coal mining waste varies between 0.3 to 0.7 Mg for each Mg of coal mined in the Upper Silesian Coal Basin (GZW) [2,3]. The waste material is generated when mining the rock mass, winning coal, and its processing. The coal mining [4] waste stored in heaps mainly includes silstone (40–98%), mudstone (2–40%), sandstone (0–33%), coal shale (2–25%), and hard coal (3–10%). This waste mostly consists of mineral matter in variable amounts, with organic matter accounting for up to 15% [5]. The minerals mostly comprise clay minerals (50–70%), quartz (20–30%), and other minerals (10–20%), including chlorite, pyrite, siderite, ankerite, gypsum, and jarosite [5]. The composition of coal mine waste depends on the geological composition of the basin and the development of preparation technologies [6]. Coal mining wastes are treated to a small extent as a source of mineral raw materials used in the economy [2]. Mining waste was and still continues to be stored in the form of heaps, dumping grounds, or sedimentation ponds. Two hundred and twenty-six [6] such facilities have been identified in the Silesian Voivodeship (Figure 1). Coal waste heaps and dumping grounds excluded from social and economic use may negatively influence the environment in the area of their origin (pollution of soil, underground, and

surface waters). Dumping grounds containing thermally active coal waste pose a threat to inhabitants due to high surface temperature and loosening of the embankment material. Oxidation of organic matter from waste can lead to self-heating and emission of pollutants, and can negatively affect air quality in the vicinity of the dumping ground [7,8].



Figure 1. Distribution of dumping grounds within the Silesian Voivodeship (Poland).

Coal and barren sedimentary rocks contain varying concentrations of naturally radioactive material (NORM) including uranium (^{238}U), thorium (^{232}Th), and potassium (^{40}K) [9,10]. Carboniferous rocks erode easily when exposed to water and air. Radionuclides (^{226}Ra , ^{232}Th , ^{40}K) contained in coal mineral matter and coal mining waste may have a potential negative impact on the environment in the heap vicinity [11]. The element erosion processes in barren rock dumping sites may have an indirect impact on the environment. Uranium and thorium erode easily in an acidic environment and pose a potential threat to humans [12,13]. Rock weathering contributes to the geochemical mobilization of uranium, during which uranium oxidizes (from +IV valence state to +VI), and is easily leached in this form. REEs present in hard coal and coal mining waste may be of economic significance. Coal deposits enriched in REEs are researched by many authors [14–19]. The pyrite, present in mining waste, under hypergenic conditions, is subject to weathering and the weathering products can react with REE-containing minerals, e.g., phosphates (monazite, xenotime) or aluminophosphates of the crandallite group [20]. Under hypergenic conditions, minerals containing lanthanides are not subject to weathering. In contrast, feldspars and biotite present in mining waste degrade, releasing REEs into the environment (e.g., Ce^{3+} is oxidised to Ce^{4+} and yttrium can be transported long distances from the waste dumping site, lanthanum occurs as La^{3+} and readily forms compounds with carbonates, silicates, and oxides) [21].

The studied coal mining waste mainly includes waste material deposited in the floor and the roof of a coal bed together with mineral interlayers brought to the surface together with the mined and processed material. This research was conducted to determine the content of REE, U, and Th in coal mining waste obtained from the bottom dumping ground layer, which is partially thermally active. We have identified the mineral phases being carriers of these elements. We measured the concentrations of radionuclides in hard coal and coal mining waste to determine their potential impact on the environment and the health of the population.

2. Research Materials and Methods

The research covered coal mining waste from the surface layer of a heap originating from a hard coal mine belonging to the Polska Grupa Górnicza (Polish Mining Group). The heap of mining waste is partially thermally active in some of its parts. The rocks coexisting with coal beds, originating from roofs, floors, and interlayers, are genetically varied and characterized by variable mineral and chemical composition. The following samples were taken for analyses: siltstone, mudstones (with admixtures of coal), sandstones, and burnt coal shales. Mudstones and sandstones are the most abundant in the coal mining waste deposited on the heap. Samples of hard coal deposited in the heap were also collected for analysis. A total of 28 samples were taken, including mining waste (20) and hard coal (8). The samples come from the heap surface and a depth of up to 0.7 m. The lower part of the heap is directly adjacent to residential houses and is not covered with vegetation. The duplicate method was used for sampling; it consists of taking a sample and its duplicate from the same test site and analyzing them twice (balanced strategy) [22]. Eight mining waste samples and two hard coal samples (a proper sample and a duplicate) were selected for further research. These samples were selected due to their low macroscopic variation, the remaining samples were rejected. The following labelling was used for the analyzed samples in Tables 1–4: 1, 1A-siltstone; 2, 2A-sandstone; 3, 3A-mudstone; 4, 4A-burnt coal shale (red); 5, 5A-hard coal. Samples labelled 1–4 represent the surface of the heap, whereas samples 1A–4A were taken from a depth of approximately 0.7 m. Samples 5 and 5A represent hard coal.

The measurements of natural radioactivity in the analyzed samples were performed using a gamma spectrometer. This spectrometer is equipped with a high purity germanium detector (GC2018, Mirion Technologies (Canberra), Inc. (Meriden, CT, USA)), with a crystal diameter of 60.7 mm and an electrically powered cryostat Cryo-Pulse 5 from Mirion Technologies (Canberra), Inc. (Meriden, CT, USA). The detector is shielded with an 11 cm thick low-background lead shield (Ortec). The HPGe detector has a relative efficiency of 20%. The full width at half maximum (FWHM) for 1.332 MeV gamma line from ^{60}Co is equal to 1.71 keV and Peak-to-Compton (P/C) ratio of 53.8:1. Data analysis and acquisition was performed using Genie 2000 software (V3.4.1). The analyzed samples were dried, ground, mixed, placed in Marinelli containers, and left for a month to achieve a radioactive equilibrium between ^{226}Ra , ^{228}Ra and their derivatives. The activities of the analyzed radionuclides were calculated on the basis of a standard prepared from certificated materials obtained from the Central Laboratory for Radiological Protection (CLOR) in Poland. The concentrations of ^{228}Ra and ^{226}Ra isotopes in the analyzed samples were calculated as a weighted mean from the activities of ^{228}Ac (338.3, 911.1 keV) and ^{214}Pb (295.2, 351.9 keV), ^{214}Bi (609.3, 1120.3 keV), respectively. The activity concentration of the ^{40}K isotope was assessed based on the 1460.8 keV gamma line. Radionuclide concentrations were measured once in the studied samples.

REE (La, Ce, Nd, Sm, Eu, Tb, Yb, Lu), U, and Th contents in the samples were determined by instrumental neutron activation analysis (INAA) at Activation Laboratories Ltd. (Ancaster, ON, Canada) using a 2MW Pool research reactor. Gamma radiation was measured using Ge ORTEC and CANBERRA detectors. Rare earth elements such as Pr, Gd, Dy, Ho, Er, and Tm + Y were determined by fusing the INAA, ICP-MS (Inductively Coupled Plasma Mass Spectrometry), and ICP-OES (Inductively Coupled Plasma Atomic Emission Spectroscopy) methods (Activation Laboratories Ltd., Ancaster, ON, Canada). REY, U, and Th concentrations were analyzed twice for each sample.

A Philips XL 30 ESEM/TMP microscope software (fully MS Windows NT compatible) with an EDS unit was used to determine the chemical composition of the mineral phases present in the coal waste samples by scanning electron microscopy. The accelerating voltage of the electron beam was 15–20 kV and the current was 20 nA. Tests were performed using preparations embedded in epoxy resin and polished.

3. Results and Discussion

3.1. Radionuclides

The $^{226,228}\text{Ra}$ and ^{40}K concentrations, U and Th content are presented in Table 1. The concentrations of the analyzed radionuclides in the investigated samples are variable. Lower values of $^{226,228}\text{Ra}$ and ^{40}K isotopes were observed in hard coal and sandstone samples. High concentrations of the analyzed isotopes were observed in the siltstone sample. Lower concentrations of radionuclides were observed for particular samples taken from the surface layer of the dump. The reverse trend was observed only in the case of the fired burnt shale samples.

Table 1. The activity concentrations in [Bq/kg] of ^{226}Ra , ^{228}Ra , ^{40}K , and content in [mg/kg] of U and Th in coal waste.

Sample Number	^{226}Ra [Bq/kg]	^{228}Ra (^{228}Ac) [Bq/kg]	^{40}K [Bq/kg]	U [mg/kg]	Th [mg/kg]	
Siltstone	1	49.5 ± 1.7	44.5 ± 1.0	749 ± 12	4.3	11.3
	1A	112.3 ± 4.1	54.2 ± 1.0	862 ± 13	9.2	11.9
Sandstone	2	9.3 ± 0.3	7.6 ± 0.2	148 ± 3	0.9	2.2
	2A	24.4 ± 0.9	12.5 ± 0.4	207 ± 4	2.1	3.1
Mudstone	3	39.0 ± 1.3	27.7 ± 0.6	761 ± 12	3.3	7.2
	3A	70.8 ± 2.6	57.6 ± 1.2	1008 ± 16	5.9	2.9
Burnt coal shale	4	69.9 ± 2.3	47.3 ± 0.9	769 ± 12	5.8	11.6
	4A	12.0 ± 0.5	10.6 ± 0.3	192 ± 4	1.1	7.8
Hard coal	5	20.3 ± 0.7	7.7 ± 0.3	64 ± 2	1.4	1.9
	5A	24.1 ± 0.9	15.1 ± 0.4	168 ± 4	2.1	3.9

The activity concentrations of $^{226,228}\text{Ra}$ and ^{40}K in hard coal are within the range of values found in literature data for GZW coals [23]. In coal mining rocks the concentrations of radionuclides vary greatly depending on the type of waste. The highest uranium concentrations were found in siltstone and mudstone samples, whereas the lowest ones were found in sandstone samples (Table 1). The most variable concentration of U was found in the samples of siltstone, mudstone and burnt coal shale. In the siltstone samples, the Th concentration (11.3–11.9 mg/kg) is at a similar level. The largest variation in Th content was found in samples of mudstone (2.9–7.2 mg/kg) and burnt coal shale (7.8–11.6 mg/kg).

In coal samples from the heap, U and Th concentrations are within the range determined for GZW hard coals; i.e., for U < 0.1–8.5 mg/kg and for Th 0.1–14.9 mg/kg [24,25]. In European hard coals, the concentration ranges for U and Th are 5–29 mg/kg and 5–65 mg/kg, respectively [25]. Chinese coals normal exhibit background values for trace elements except, for example, Th (5.84 mg/kg) [26]. Some of these coals can be enriched in both U (54.5 to 100 mg/kg) and Th (up to 19.3 mg/kg) [27–29]. South African coals also contain U in a wide range of concentrations, varying from 2.9 to 199 mg/kg [30].

In order to assess the interdependence between the analyzed isotopes, the Pearson correlation analysis was performed (Figure 2). The ^{238}U and ^{232}Th concentrations were calculated based on U and Th content (Table 1). The correlation coefficient values range from +1 (perfect positive correlation) to −1 (perfect negative correlation). On the other hand, a correlation coefficient close to zero showed no linear correlation [31]. The values of this coefficient between −1 and 1 indicate the degree of linear dependence between the variables.

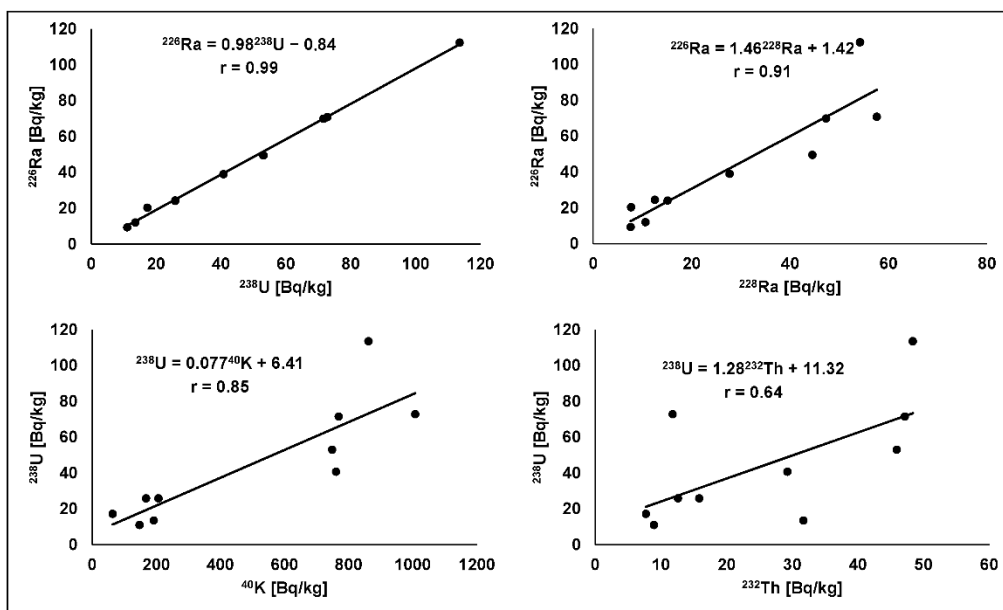


Figure 2. The correlation between pairs: ^{226}Ra - ^{238}U , ^{226}Ra - ^{228}Ra , ^{238}U - ^{40}K , ^{238}U - ^{232}Th .

A full correlation between activity concentrations of the daughter ^{226}Ra and parent ^{238}U isotope was observed ($r = 0.99$). Very high correlation between pairs: (^{226}Ra - ^{228}Ra : $r = 0.91$), (^{238}U - ^{40}K : $r = 0.85$) was noted. A moderate correlation between ^{238}U and ^{232}Th ($r = 0.64$) was observed. Previous studies [32] also showed a very high correlation between pairs: (^{238}U - ^{228}Ra), (^{238}U - ^{40}K) for different feed hard coal samples (hard coal, culm, and silt), and for ^{238}U and ^{226}Ra isotopes, the correlation was high.

Waste deposited in landfills sometimes showed a high radioactive content and may have a negative impact on the environment. Therefore, the radiological risk from gamma radionuclides present in the landfills was investigated. The following risk indicators: radium equivalent activity (R_{aeq}), external hazard index (H_{ex}) were assessed [33] on the basis of equations:

$$R_{\text{aeq}} = ^{226}\text{Ra} + 1.43 \cdot ^{232}\text{Th} + 0.077 \cdot ^{40}\text{K}, \tag{1}$$

$$H_{\text{ex}} = \frac{^{226}\text{Ra}}{370} + \frac{^{232}\text{Th}}{259} + \frac{^{40}\text{K}}{4810}, \tag{2}$$

where: concentrations of ^{40}K , ^{226}Ra , ^{232}Th isotopes are expressed in Bq/kg.

R_{aeq} should be lower than 370 Bq/kg [34] and H_{ex} value less than or equal to unity to limit the external gamma radiation dose below 1.5 mSv/y [33,35].

The absorbed dose rate in [nGy/h] from gamma radiation at a high of 1m above the ground level can be calculated as follows [34,36]:

$$D \left[\frac{\text{nGy}}{\text{h}} \right] = 0.462 ^{226}\text{Ra} + 0.604 ^{232}\text{Th} + 0.0417 ^{40}\text{K}, \tag{3}$$

The annual effective dose rate [36] was calculated based on Equation:

$$\text{ED} \left[\frac{\text{mSv}}{\text{y}} \right] = D \times 0.7 \times 0.2 \times 8760 \times 10^{-6}, \tag{4}$$

In dose calculation, according to UNSCEAR [36] report, the conversion coefficient from the absorbed dose to the effective dose equal to 0.7 [Sv/Gy] and the outdoor occupancy factor equal to 0.2 were used.

The values of radium equivalent activity (R_{aeq}), external hazard index (H_{ex}) (Table 2), are lower than the limits.

Table 2. The calculated values of Radium equivalent activity (R_{eq}), external hazard index H_{ex} , air absorbed dose rates D [nGy/h], and annual effective dose ED [mSv/y].

Sample Number	R_{eq} [Bq/kg]	H_{ex}	D [nGy/h]	ED [mSv/y]
Siltstone	1	173	0.5	83.5
	1A	248	0.7	117.0
Sandstone	2	33	0.1	16.7
	2A	58	0.2	28.2
Mudstone	3	139	0.4	68.2
	3A	165	0.4	82.8
Burnt coal shale	4	197	0.5	93.6
	4A	72	0.2	33.4
Hard coal	5	36	0.1	15.3
	5A	60	0.2	28.6

The absorbed dose in the air reaches the value of 117.0 [nGy/h]. According to the report [36], the average absorbed dose rate in the air outdoors from terrestrial gamma radiation is equal to 60 [nGy/h]. The effective radiation dose reaches the value of 0.14 mSv/y, which is below the limit of 1 mSv/y [36].

3.2. REE

Table 3 presents the results of REY determinations in coal waste samples.

In coal samples, REE concentrations were determined from 15.6 mg/kg to 15.7 mg/kg. The low REE content (15.7 mg/kg) in Polish hard coal is confirmed by studies by Calusz-Motoszko and Białecka [37] and Żelazny et al. [38], who report REE contents in the range of 6–60 mg/kg. Coals generally contain REE in the range up to 69 mg/kg [39]. Anomalies of $\Sigma REE + Y$ in hard coal have been found in Russia, Poland, Romania, the United States, and China [40]. Coal from China [29,41] and India (100–200 mg/kg) was found to have high concentrations of REE (172–232.2 mg/kg) [42]. Both hard coal and barren rocks can be enriched in REE [16].

Coal mining wastes are clearly enriched in lanthanides; these include clays, which contain REY ranging from 245.5 mg/kg to 261.1 mg/kg (Table 3).

Based on the geochemical classification of Seredin and Dai [16], the REY in hard coal and coal waste is classified into light (LREY-La, Ce, Pr, Nd, and Sm), medium (MREY-Eu, Gd, Tb, Dy, and Y), and heavy (HREY-Ho, Er, Tm, Yb, and Lu) groups (Table 3).

La, Ce, Nd, Eu, Sm, Yb, and Lu concentrations determined in the siltstone samples are consistent with the results of the study by Kokowska-Pawłowska [43]. The lowest REE content (135.2–180 mg/kg) was determined in burnt coal shale (Table 3).

When studying mining waste Nowak and Kokowska-Pawłowska (2017) [44] found that the REE_s content varies depending on the degree of thermal transformation of the waste. In thermally unprocessed and moderately processed waste, the average REE_s content is similar, ranging from 184.0 mg/kg to 187.5 mg/kg. According to Nowak and Kokowska-Pawłowska (2017) [44], higher content of REE_s (225.6 mg/kg) is found in mining waste from the highly thermally processed zones. In these wastes, they found higher concentrations of La (40.1 mg/kg), Nd (32.9 mg/kg), Sm (5.8 mg/kg), and Y (55.6 mg/kg), compared with the waste from the thermally unprocessed and moderately processed zones.

The determined lanthanide concentration values for coal waste samples were normalized to NASC (North American Shale Composites) [45] (Table 4). Anomaly ratio values below 0.8 indicate a negative anomaly and those above 1.2 indicate a positive anomaly [45,46]. The values of REY concentrations normalized to NASC are indicative of the studied coal mining waste being enriched in LREY. The mean numerical values of the Ce/Ce_{NASC} ($Ce/Ce_{NASC} = 0.5La_{NASC} + 0.5Pr_{NASC}$) [47] (3.5–5.8) anomaly ratio are indicative of a positive anomaly in the studied coal waste samples (Table 4). The values of the Ce/Ce_{NASC} (1.3–3.6) anomaly ratio vary the most in the burnt shale samples. This is due to significant variation in concentrations of REY determined for samples 4 and 4A.

The degree of shale thermal transformation is one of the factors that may influence its heterogeneity in chemical and mineral composition.

Table 3. The concentrations in [mg/kg] of REY in coal waste samples.

Element	Sample Number									
	Silstone		Sandstone		Mudstone		Burnt Coal Shale		Hard Coal	
	1	1A	2	2A	3	3A	4	4A	5	5A
La	50.3	52.2	36.4	39.1	31.6	36.8	37.7	25.2	1.9	2.1
Ce	111.0	114.0	87.2	91.2	76.5	99.2	88.2	67.3	5.5	5.3
Pr	12.5	13.8	10.3	11.8	8.5	9.9	10.2	7.7	0.8	0.8
Nd	42.5	49.8	42.4	49.5	30.8	34.6	26.7	21.8	3.6	3.5
Sm	8.2	9.8	7.8	8.4	5.1	5.5	7.2	6.1	0.8	0.7
Eu	1.3	1.6	1.6	1.6	1.1	1.3	0.7	0.3	0.8	0.6
Gd	7.3	7.8	6.1	7.6	3.8	4.5	3.1	2.5	0.7	0.7
Tb	0.9	0.9	1.1	1.1	0.6	0.8	0.4	0.2	0.1	0.1
Dy	4.6	5.8	4.2	5.1	3.3	3.6	2.8	2.1	0.6	0.7
Ho	1.2	1.1	0.6	0.9	0.7	0.9	0.1	0.1	0.1	0.1
Er	2.9	2.1	1.8	2.2	2.3	2.0	1.2	0.8	0.4	0.4
Tm	0.1	0.1	0.1	0.1	0.1	0.2	0.1	0.1	0.1	0.1
Yb	2.4	2.5	2.0	2.3	1.9	2.3	1.4	0.9	0.3	0.5
Lu	0.3	0.1	0.3	0.3	0.3	0.3	0.2	0.1	0	0.1
Y	29.1	31.3	23.6	27.8	30.3	34.2	21.5	18.6	4.4	4.6
∑REE	245.5	261.6	201.9	221.2	166.3	201.9	180.0	135.2	15.6	15.7
LREY	224.5	239.6	184.1	200.0	152.5	186.0	170.0	128.1	12.6	12.4
MREY	43.2	47.4	36.6	43.2	39.1	44.4	28.5	23.7	6.6	6.4
HREY	6.9	5.9	4.8	5.8	5.3	5.7	3.0	2.0	0.9	1.2

Table 4. Anomaly coefficients of NASC-normalized concentrations of individual lanthanides.

Anomaly Coefficient	Sample Number									
	Silstone		Sandstone		Mudstone		Burnt Coal Shale		Hard Coal	
	1	1A	2	2A	3	3A	4	4A	5	5A
Ce/Ce _{NASC}	5.7	5.8	4.5	4.7	3.9	5.1	4.5	3.5	0.6	0.3
La/Yb _{NASC}	16.2	16.8	11.7	12.6	10.2	11.8	12.1	8.1	0.6	0.4
La/Sm _{NASC}	8.4	8.7	6.1	6.5	5.3	6.2	6.3	4.2	0.5	0.6
Sm/Yb _{NASC}	2.6	3.2	2.5	2.7	1.6	1.8	2.3	2.0	1.4	0.7
Eu/Eu _{NASC}	5.9	7.2	7.2	7.2	5.0	5.9	3.1	1.3	3.6	2.7

REE+Y [mg/kg] Concentrations in Shales (NASC) ¹										
Y	La	Ce	Pr	Nd	Sm	Eu	Gd	Tb	Dy	Ho
27	31.1	67.033	7.9	30.4	5.98	1.25333	5.5	0.85	5.75	1.2

¹ Migaszewski and Gałuszka, 2019 [45].

Coal waste is enriched in LREY and La/Yb_{NASC} (8.1–16.8) ratio is normalized, which is indicative of strong lanthanide fractionation.

Graphs showing the REY concentration values normalized to NASC in coal waste are presented in Figure 3.

Curves representing REY concentrations normalized to NASC indicate a large variation in the lanthanides in the investigated coal mining waste samples. The strong anomaly of Ce and Eu in the tested samples from the coal waste heap is probably due to the nature of these samples. This anomaly is most common in coal rocks, as confirmed by the studies of Serdin and Dai (2016) [16]. A strong positive Eu anomaly may be the result of the high temperature on the heap (even up to 200 °C) and the chemical composition of the coal mine waste (iron sulfides). The coals with positive Eu anomalies are characterized by a

high pyrite content [47]. Heating inside a coal waste dump is typically highly variable with temperatures ranging from ambient to >500 °C [48]. Coal wastes deposited on the dump undergo a number of processes which can completely change their initial chemical or mineral composition [5]. The normalized Ho/Ho_{NASC} content in coal mine waste samples is from 1.0 (silstone) to 0.08 (burnt coal shale and hard coal). Sandstone (2, 2A) and mudstone (3, 3A) samples are the most stable as the concentration curves of REY normalized to NASC in these waste types are similar. The greatest variation in normalized REY concentration values was found in the burnt coal shale (4 and 4A).

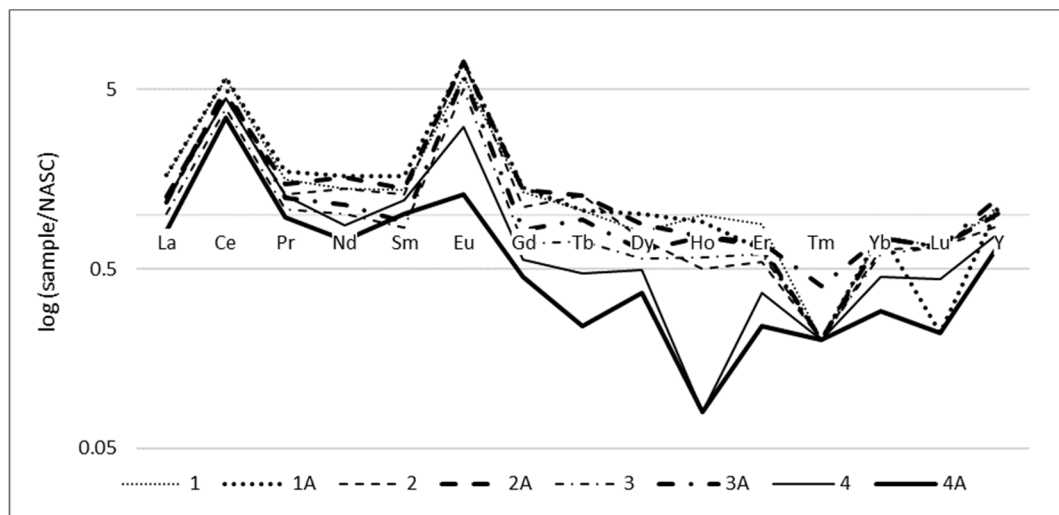


Figure 3. Characteristic of REY normalized to NASC in the studied coal mine waste samples.

Coal samples (5, 5A) normalized to NASC (Figure 4) are indicative of a marked increase in Eu compared to the other normalized lanthanide concentrations. The value of the normalized $\text{Eu}/\text{Eu}_{\text{NASC}}$ ($\text{Eu}/\text{Eu}_{\text{NASC}} = \text{Eu}_{\text{NASC}} / (\text{Sm}_{\text{NASC}} \cdot \text{Gd}_{\text{NASC}})^{0.5}$) [49] anomaly ratio is 2.7–3.6.

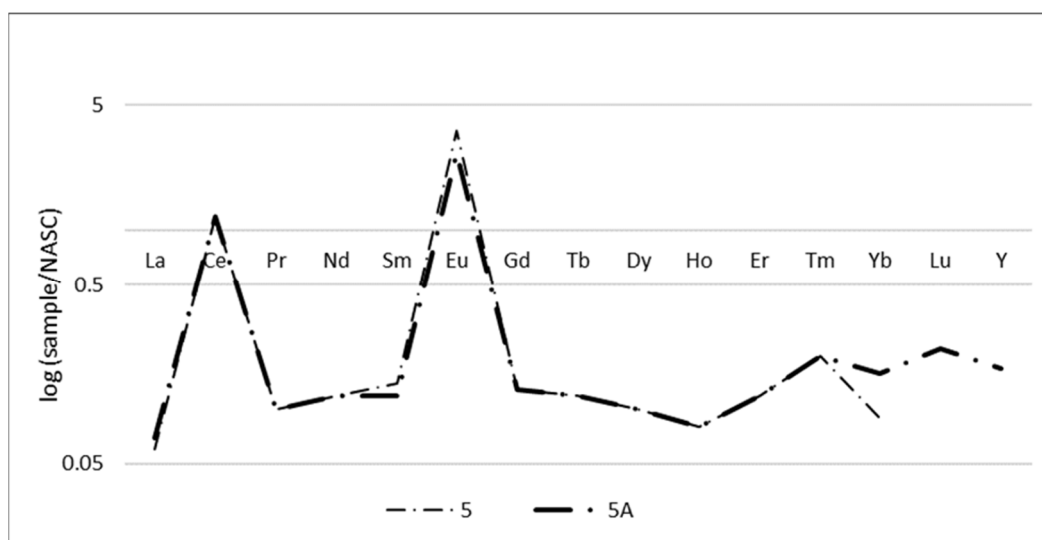


Figure 4. Characteristic of REY normalized to NASC in the studied hard coal samples.

The Y concentration (4.4–4.6 mg/kg) in the coal samples is low compared to the coal waste samples (31.3–18.6 mg/kg). The lowest Y content was found in the burned shale samples and the highest in the silstone samples (Table 3). The Y content in all coal mining waste samples was correlated with the LREY and HREY content. Strong correlations were

found between Y concentration and HREY content ($r = 0.91$), and with LREY ($r = 0.92$) (Figure 5). All coal waste samples were analyzed for correlation. According to Leticariu et al. [50], the Y/Ce ratio can be used to predict enrichment in REY. In the analyzed coal waste samples, the Y/Ce ratio is in the range of 0.3–0.5. Coal samples exhibited a higher value of the Y/Ce ratio (0.8–0.9). In the investigated coal waste samples, the relationship between Y concentration and Ce concentration is also moderate ($r = 0.63$).

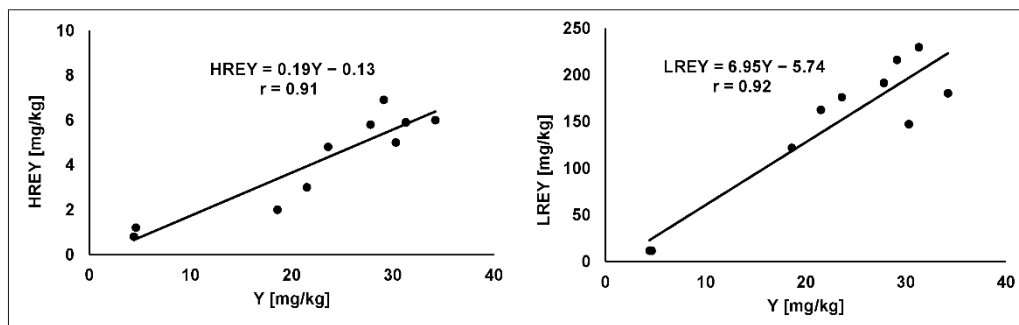


Figure 5. Correlation graphs between the concentration of Y and the concentration of HREY and LREY in coal waste samples.

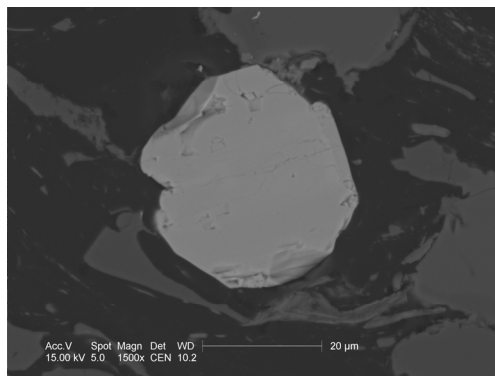
3.3. Phase Composition

In the coal samples, rare earth phosphates, mainly monazite (Ce, La, Nd, Th, U, Pr)[PO₄], are also the sources of REY, U, and Th. Xenotime [YPO₄] was rarely found and therefore cannot be considered as a source of actinides in hard coal stored in heaps.

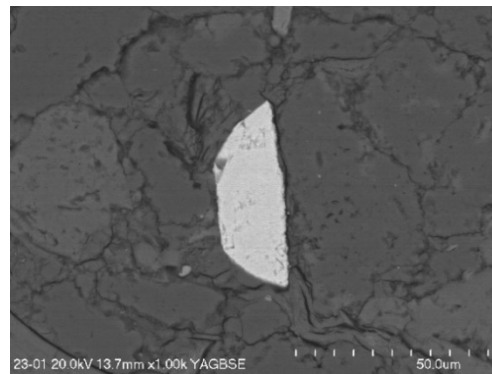
Monazite, which is a carrier of REY, U, and/or Th, was also identified in coal waste samples. The identified monazite grains can be divided into 3 types with varied morphology and varied content of identified rare earth oxides, uranium and thorium (Figure 6a–f). All types of monazite were found in the mudstone and silstone samples, including solid and compact grains, where cracks were rarely observed (Figure 6a,b). Monazite grains exhibit high concentrations of ThO₂ (>14%) and much lower concentrations of UO₂ (up to 1.72%). These grains are characterized by concentrations of Nd, Pr, and Sm oxides.

The second monazite type includes highly fractured, irregularly shaped grains with ThO₂ concentration not exceeding 8% (Figure 6c,d). Lower content of La₂O₃ and Ce₂O₃ was found in monazite compared to grains of the first type. No UO₂ was found in this monazite type, and the ThO₂ concentration does not exceed 7%.

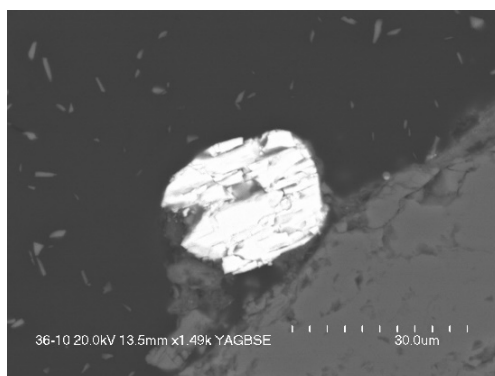
The third monazite type is characterized by partially or strongly crushed grains, some of which exhibit traces of dissolution (Figure 6e). Monazite of this type contains either uranium or thorium. The UO₂ (up to 0.34%) and ThO₂ (up to 1%) oxide content is low compared to monazite of the first and second types. The monazite grains exhibit higher La₂O₃ and Ce₂O₃ concentrations, which is at a similar level as in monazite of the first type. Gd₂O₃ content was determined in these monazite grains and its concentration was found to be in the range of 0.76–1.51%.



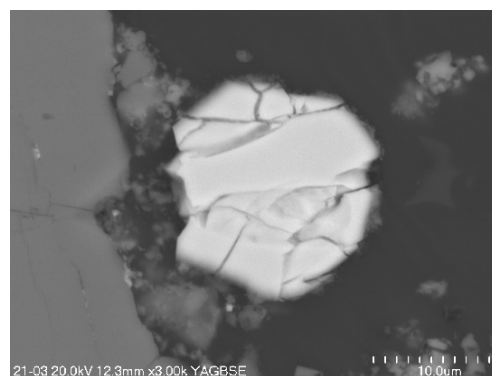
(a) P_2O_5 -18.63%; La_2O_3 -10.48%; Ce_2O_3 -37.61%; Pr_2O_3 -2.25%; Nd_2O_3 -12.66%; Sm_2O_3 -0.77%; UO_2 -1.17%; ThO_2 -16.43%



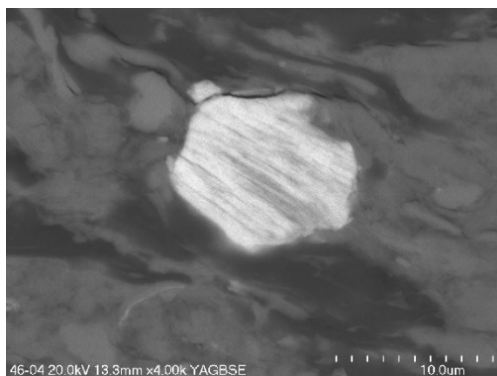
(b) P_2O_5 -27.88%; La_2O_3 -7.71%; Ce_2O_3 -31.15%; Pr_2O_3 -1.33%; Nd_2O_3 -9.26%; Sm_2O_3 -0.16%; UO_2 -1.03%; ThO_2 -21.48%



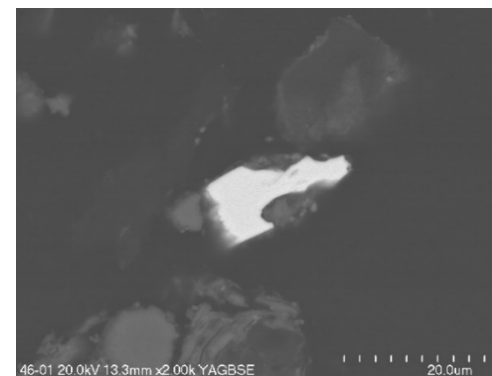
(c) P_2O_5 -2.54%; CaO -3.28%; Al_2O_3 -5.10%; SiO_2 -5.34%; K_2O -0.84%; La_2O_3 -6.62%; Ce_2O_3 -21.67%; Nd_2O_3 -6.83%; Sm_2O_3 -0.55%; ThO_2 -7.23%



(d) P_2O_5 -39.68%; Al_2O_3 -3.67%; SiO_2 -3.41%; La_2O_3 -9.07%; Ce_2O_3 -26.48%; Pr_2O_3 -1.46%; Nd_2O_3 -8.26%; Sm_2O_3 -1.26%; ThO_2 -6.71%

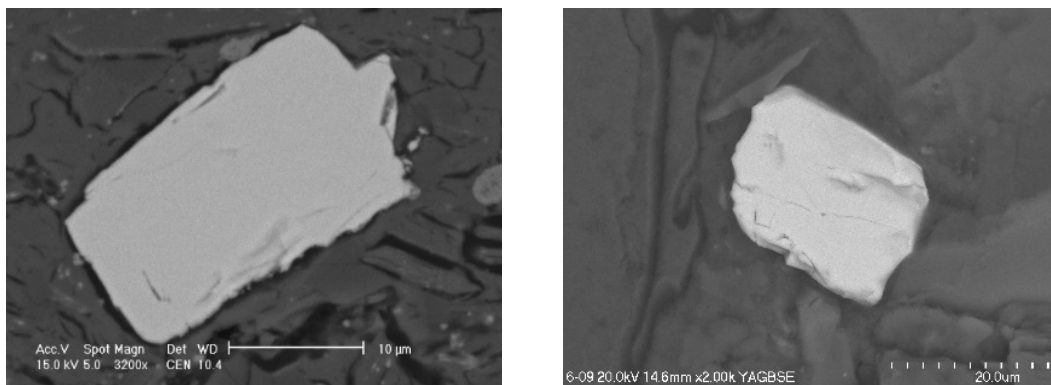


(e) P_2O_5 -37.11%; CaO -2.17%; SiO_2 -0.81%; La_2O_3 -1.90%; Ce_2O_3 -33.67%; Pr_2O_3 -2.17%; Nd_2O_3 -9.40%; Sm_2O_3 -1.13%; Gd_2O_3 -1.51%; UO_2 -0.13%



(f) P_2O_5 -33.55%; Al_2O_3 -0.98%; SiO_2 -6.49%; CaO -1.08%; La_2O_3 -12.42%; Ce_2O_3 -32.66%; Nd_2O_3 -9.57%; Sm_2O_3 -2.33%; ThO_2 -0.92%

Figure 6. Cont.



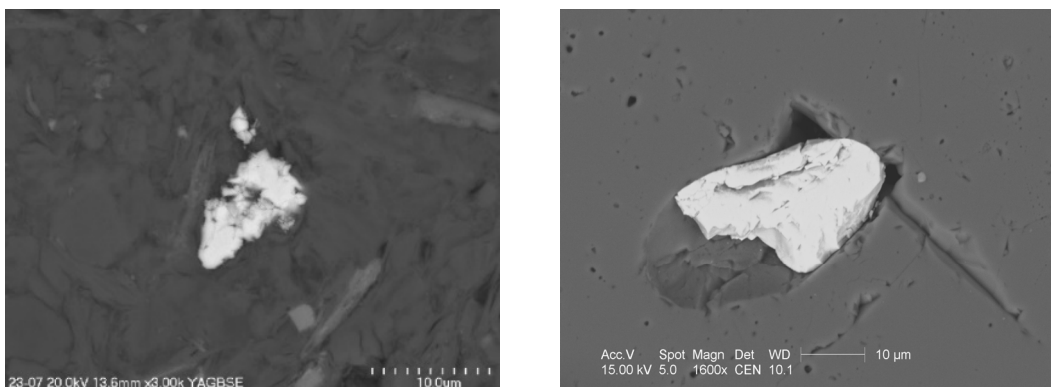
(g) P_2O_5 -36.26%; SiO_2 -1.07%; K_2O -0.24%; La_2O_3 -9.12%;
 Ce_2O_3 -33.77%; Pr_2O_3 -1.76%; Nd_2O_3 -10.18%; Sm_2O_3 -0.98%;
 Gd_2O_3 -0.76%; UO_2 -0.65%; ThO_2 -5.21%;

(h) P_2O_5 -36.36%; La_2O_3 -11.16%; SiO_2 -1.24%; Fe_2O_3 -
 3.41%; Ce_2O_3 -32.87%; Pr_2O_3 -1.38%; Nd_2O_3 -9.46%;
 Sm_2O_3 -1.18%; UO_2 -0.07%; ThO_2 -2.87%;

Figure 6. Photographs of monazite particles in coal waste samples (a,c,e—silstone; b,d,f—mudstone; g,h—sandstone) obtained using BSE SEM technique.

In the sandstone samples, monazite grains of the first type were observed, which are weak in UO_2 and ThO_2 compared to the mudstone and silstone samples (Figure 6g,h).

In the burnt coal shale samples monazite grains of the first and third type were found (Figure 7). The chemical composition of monazite varies a lot, which results from the thermal transformation of the coal waste. Variable concentrations of UO_2 (0.36–1.38%) and ThO_2 (2.46–10.39%) were found in monazite. The concentrations of La_2O_3 , Ce_2O_3 , and Nd_2O_3 also vary a lot.



P_2O_5 -37.25%; Al_2O_3 -4.00%; SiO_2 -6.61%;
 MgO -0.46%; CaO -2.08%; K_2O -0.34%;
 TiO_2 -6.80%; La_2O_3 -6.17%; Ce_2O_3 -21.16%;
 Nd_2O_3 -8.52%; Sm_2O_3 -1.65%; Gd_2O_3 -1.12%;
 UO_2 -1.38%; ThO_2 -2.46%;

P_2O_5 -43.73%; Al_2O_3 -0.33%; SiO_2 -1.88%;
 CaO -1.38%; La_2O_3 - 8.44%; Ce_2O_3 -28.41%;
 Nd_2O_3 -2.45%; Sm_2O_3 -0.92%; Gd_2O_3 -1.71%;
 UO_2 -0.36%; ThO_2 -10.39%;

Figure 7. Photographs of monazite particles in burnt coal shale samples using the BSE SEM technique (scale—10 µm).

The chemical composition of the xenotime (Y) in REY exhibited variable contents of MREY and HREY, as well as UO_2 and/or ThO_2 , were found (Figure 8). It was mainly observed in the silstone (Figure 8a) and mudstone samples (Figure 8b). Xenotime grains are rarely found in sandstone (Figure 8c) and burnt coal shale samples (Figure 8d).

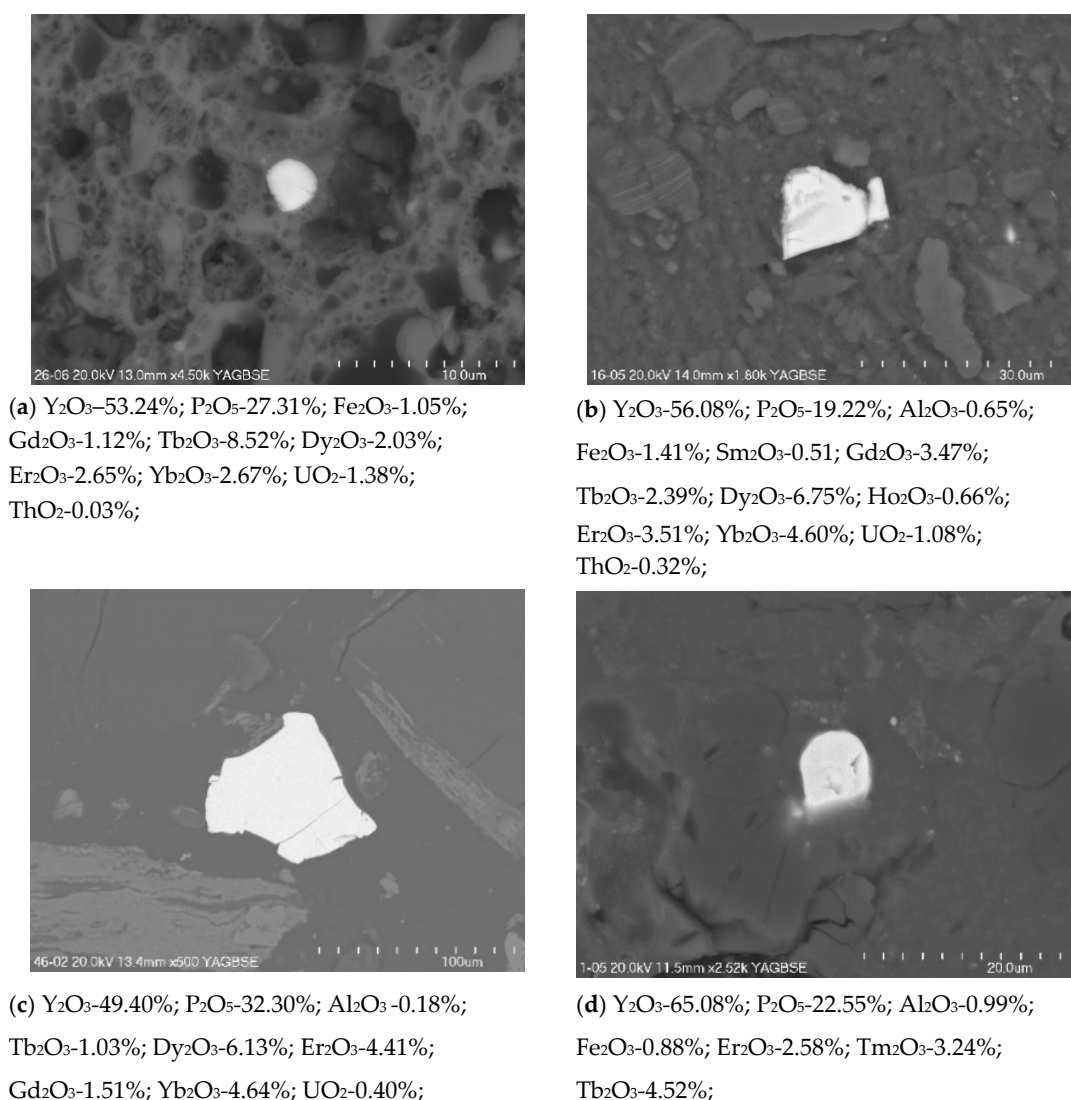


Figure 8. Photographs of xenotime (Y) particles in coal samples (a—silstone; b—mudstone; c—sandstone; d—burnt coal shale) obtained using BSE SEM technique.

The observed xenotime grains have Y_2O_3 content ranging from 49.61% to 56.08%. Among LREY and MREY, samarium and holmium occur sporadically with concentrations not exceeding 0.70%. The chemical composition of xenotime exhibited varied oxide contents: Gd_2O_3 (1.12–3.47%), Tb_2O_3 (2.39–8.52%), Dy_2O_3 (2.03–6.75%), and Yb_2O_3 (2.67–4.60%). Higher concentrations were recorded for UO_2 (0.68–1.38%; max. 6.83%) than ThO_2 (0.03–0.32%). The strong correlation between Y and HREY and LREY concentration (Figure 5) suggests that the rare earths are bound by xenotime and another substance, probably coal organic matter, which has often been found in coal mining waste (silstone and mudstone).

Numerous very fine agglomerations of rare earth phosphates (monazite and occasionally xenotime) have been found in hard coal. According to Seredin and Dai [16], and Ramakrishna [39], REE-rich minerals in hard coal mainly include fine-grained autogenous minerals (including REE-rich aluminum phosphates and sulphates, phosphates, and carbonates), as well as organic compounds. Dai et al. (2012) [51] found LREY associations in goyazite and gorceixite, MREY and HREY in boehmite, and some indications of MREY and HREY associations in accessory minerals. In addition to REE-rich minerals monazite and zircon, Hower et al. [52,53] found minerals containing rare earth elements on the nanoscale (monazite interlaid with kaolinite 10 nm to 1 μ m). According to Pluta et al. [54], uranium

is also found in secondary phosphates found on the cleavage surface of clay minerals in coal and is found in association with iron and zinc sulfides, and barite.

4. Conclusions

Preliminary results derived from a statistically small number of mining waste samples allow limited conclusions to be drawn, and further research in this area is needed.

The varying values of REY, U and Th concentrations in coal mining waste are due to the heterogeneity in chemical and mineral composition of the material deposited on the heap.

Monazite (Ce) in coal waste material on heaps is the main source of LREY. Quantitatively, xenotime (Y) is less important than monazite. Monazite cannot be the sole REY carrier like xenotime, which contains variable amounts of HREY (the positive correlation between Y concentration and HREY concentration is insufficient to determine the source of radioactivity). It might be assumed that rare earth phosphates in the studied coal mining waste take the form of very fine agglomerations in other minerals of Carboniferous rocks.

The analyzed barren rocks were characterized by variable strength of radioactive activity of the isotopes, with the highest values found in siltstone and mudstone samples.

With the calculated radiological indices, the environmental impact of the coal waste heap and its influence on the health of the local population may be judged insignificant. Please note, however, the variability within the same type of waste (higher values in waste deposited in the heap profile down to the depth of 0.7 m), which requires further research.

Author Contributions: D.S.-D. contributed to the conception of the study. A.W.-Ł., D.S.-D. contributed significantly to analysis and manuscript preparation, and wrote the manuscript. All authors have read and agreed to the published version of the manuscript.

Funding: This research received no external funding.

Data Availability Statement: The data presented in the study is available on request from the corresponding author.

Conflicts of Interest: The authors declare no conflict of interest.

References

1. GUS—Główny Urząd Statystyczny. *Statistical Yearbook of Industry—Poland*; Publisher: Warszawa, Poland, 2019.
2. Kłojzy-Karczmarczyk, B.; Mazurek, J.; Paw, K. Możliwość zagospodarowania kruszyw i odpadów wydobywczych górnictwa węgla kamiennego ZG Janina w procesach rekultywacji wyrobisk odkrywkowych. *Gospod. Surowcami Miner. MRM* **2016**, *32*, 111–134. [[CrossRef](#)]
3. Fabiańska, M.J.; Nádudvari, Á.; Ciesielczuk, J.; Szram, E.; Misz-Kennan, M.; Więclaw, D. Organic contaminants of coal-waste dump water in the Lower- and Upper Silesian Coal Basins (Poland). *Applied Geochem.* **2020**, *122*, 104690. [[CrossRef](#)]
4. Jonczy, I.; Gawor, Ł. Coal mining and post-metallurgic dumping grounds and their connections with exploitation of raw materials in the region of Ruda Śląska. *Arch. Min. Sci.* **2017**, *62*, 301–311. [[CrossRef](#)]
5. Ciesielczuk, J.; Misz-Kennan, M.; Hower, J.C.; Fabiańska, M.J. Mineralogy and geochemistry of coal wastes from the Starzykowice coal-waste dump (Upper Silesia, Poland). *Int. J. Coal G.* **2014**, *127*, 42–55. [[CrossRef](#)]
6. Marcisz, M.; Probiez, K.; Gawor, Ł. Possibilities of reclamation and using of large-surface coal mining dumping grounds in Poland. *Gospod. Surowcami Miner. MRM* **2020**, *36*, 105–122.
7. Nádudvari, Á.; Fabiańska, M.J. Use of geochemical analysis and vitrinite reflectance to assess different self-heating processes in coal-waste dump (Upper Silesia, Poland). *Fuel* **2016**, *181*, 102–119. [[CrossRef](#)]
8. Kruszewski, Ł.; Fabiańska, M.J.; Segit, T.; Kusy, D.; Motyliński, R.; Ciesielczuk, J.; Deput, E. Carbon nitrogen compounds, alcohols, mercaptans, monoterpenes, acetates, aldehydes, ketones, SF₆, PH₃, and other fire gases in coal-mining waste heaps of Upper Silesian Coal Basin (Poland)—a re-investigation by means of in situ FTIR external database approach. *Sci. Total Environ.* **2020**, *698*, 134274.
9. Lauer, N.E.; Hower, J.C.; Hsu-Kim, H.; Taggart, R.K.; Vengosh, A. Naturally Occurring Radioactive Materials in Coals and Coal Combustion Residuals in the United States. *Environ. Sci. Technol.* **2015**, *49*, 11227–11233. [[CrossRef](#)]
10. Kolo, M.T.; Khandaker, M.U.; Amin, Y.M.; Abdullah, W.H.B. Quantification and Radiological Risk Estimation Due to the Presence of Natural Radionuclides in Maiganga Coal, Nigeria. *PLoS ONE* **2016**, *11*, e0158100. [[CrossRef](#)]
11. Kozłowska, B.; Walencik, A.; Dorda, J.; Zipper, W. Radioactivity of dumps in mining areas of The Upper Silesian Coal Basin in Poland. In *EPJ Web of Conferences*; EDP Sciences: Les Ulis, France, 2012; Volume 24, p. 05006.

12. Singh, R.K.; Gupta, N.C.; Guha, B.K. pH dependence leaching characteristics of selected metals from coal ash and its impact on ground water quality. *Int. J. Chem. Env. Enginn.* **2014**, *5*, 218–222.
13. Da Silva, E.B.; Li, S.; De Oliveira, L.M.; Gress, J.; Dong, X.; Wilkie, A.C.; Townsend, T.; Ma, L.Q. Metal leachability from coal combustion residuals under different pHs and liquid/solid ratios. *J. Hazard. Mater.* **2018**, *341*, 66–74. [[CrossRef](#)]
14. Dai, S.; Li, D.; Chou, C.-L.; Zhao, L.; Zhang, Y.; Ren, D.; Ma, Y.; Sun, Y. Mineralogy and geochemistry of boehmite-rich coals: New insights from the Haerwusu Surface Mine, Jungar Coalfield, Inner Mongolia, China. *Int. J. Coal Geol.* **2008**, *74*, 185–202. [[CrossRef](#)]
15. Dai, S.; Wang, X.; Zhou, Y.; Hower, J.C.; Li, D.; Chen, W.; Zhu, X.; Zou, J. Chemical and mineralogical compositions of silicic, mafic, and alkali tonsteins in the late Permian coals from the Songzao Coalfield, Chongqing, Southwest China. *Chem. Geol.* **2011**, *282*, 29–44. [[CrossRef](#)]
16. Seredin, V.V.; Dai, S. Coal deposits as potential alternative sources for lanthanides and yttrium. *Int. J. Coal Geol.* **2012**, *94*, 67–93. [[CrossRef](#)]
17. Blissett, R.S.; Smalley, N.; Rowson, N.A. An investigation into six coal fly ashes from the United Kingdom and Poland to evaluate rare earth element content. *Fuel* **2014**, *119*, 236–239. [[CrossRef](#)]
18. Lin, R.; Howard, B.H.; Roth, E.A.; Bank, T.L.; Granite, E.J.; Soong, Y. Enrichment of rare earth elements from coal and coal by-products by physical separations. *Fuel* **2017**, *200*, 506–520. [[CrossRef](#)]
19. Arbuзов, S.; Chekryzhov, I.; Finkelman, R.; Sun, Y.; Zhao, C.; Il'Enok, S.; Blokhin, M.; Zarubina, N. Comments on the geochemistry of rare-earth elements (La, Ce, Sm, Eu, Tb, Yb, Lu) with examples from coals of north Asia (Siberia, Russian far East, North China, Mongolia, and Kazakhstan). *Int. J. Coal Geol.* **2019**, *206*, 106–120. [[CrossRef](#)]
20. Migaszewski, Z.M.; Gałuszka, A.; Dołęgowska, S. Extreme enrichment of arsenic and rare earth elements in acid mine drainage: Case study of Wiśniówka mining area (south-central Poland). *Environ. Pollut.* **2019**, *244*, 898–906. [[CrossRef](#)]
21. Kabata-Pendias, A.; Szeke, B. *Pierwiastki Śladowe w Geo- i Biosferze*; IUNG-PIB: Puławy, Poland, 2012. (In Polish)
22. Rostron, P.D.; Ramsey, M.H. Cost effective, robust estimation of measurement uncertainty from sampling using unbalanced ANOVA. *Accredit. Qual. Assur.* **2011**, *17*, 7–14. [[CrossRef](#)]
23. Róg, L. Natural radioactivity of hard coals and coal density fractions of differentiated petrografical and chemical construction. In *Prace Naukowe GIG. Górnictwo i Środowisko/Główny Instytut Górnictwa*; Main Mining Institute: Katowice, Poland, 2005; pp. 81–101. (In Polish)
24. Bojakowska, I.; Lech, D.; Wołkowicz, S. Uranium and thorium in hard and brown coals from Polish deposits. *Gospod. Surowcami Miner. MRM* **2008**, *24*, 53–65.
25. Parzenty, H.R.; Róg, L. The role of mineral matter in concentrating uranium and thorium in coal and combustion residues from power plant in Poland. *Minerals* **2019**, *9*, 312. [[CrossRef](#)]
26. Dai, S.; Ren, D.; Chou, C.-L.; Finkelman, R.B.; Seredin, V.V.; Zhou, Y. Geochemistry of trace elements in Chinese coals: A review of abundances, genetic types, impacts on human health, and industrial utilization. *Int. J. Coal Geol.* **2012**, *94*, 3–21. [[CrossRef](#)]
27. Huang, W.; Wan, H.; Finkelman, R.B.; Tang, X.; Zhao, Z. Distribution of Uranium in the Main Coalfields of China. *Energy Explor. Exploit.* **2012**, *30*, 819–836. [[CrossRef](#)]
28. Zhao, Q.; Niu, Y.; Xie, Z.; Zhang, K.; Zhou, J.; Arbuзов, S. Geochemical characteristics of elements in coal seams 41 and 42 of Heshan Coalfield, South China. *Energy Explor. Exploit.* **2019**, *38*, 137–157. [[CrossRef](#)]
29. Wei, Q.; Song, W. Mineralogical and Chemical Characteristics of Coal Ashes from Two High-Sulfur Coal-Fired Power Plants in Wuhai, Inner Mongolia, China. *Minerals* **2020**, *10*, 323. [[CrossRef](#)]
30. Ndhlalose, M.; Malumbazo, N.; Wagner, N. Coal quality and uranium distribution in Springbok Flats Coalfield samples. *J. South. Afr. Inst. Min. Met.* **2015**, *115*, 1167–1174. [[CrossRef](#)]
31. Schober, P.; Boer, C.; Schwarte, L.A. Correlation Coefficients: Appropriate Use and Interpretation. *Anesth Analg.* **2018**, *126*, 1763–1768. [[CrossRef](#)]
32. Walencik-Lata, A.; Smółka-Danielowska, D. 234U, 238U, 226Ra, 228Ra and 40K concentrations in feed coal and its combustion products during technological processes in the Upper Silesian Industrial Region, Poland. *Environ. Pollut.* **2020**, *267*, 115462. [[CrossRef](#)]
33. Lu, X.; Li, L.Y.; Wang, F.; Wang, L.; Zhang, X. Radiological hazards of coal and ash samples collected from Xi'an coal-fired power plants of China. *Environ. Earth Sci.* **2012**, *66*, 1925–1932. [[CrossRef](#)]
34. Wang, X.; Feng, Q.; Sun, R.; Liu, G. Radioactivity of Natural Nuclides (40K, 238U, 232Th, 226Ra) in Coals from Eastern Yunnan, China. *Minerals* **2015**, *5*, 637–646. [[CrossRef](#)]
35. You, M.; Hu, Y.; Lu, J.; Li, C. Evaluation of the radiological characterization in a coal-fired power plant, China. *Environ. Prog. Sustain. Energy* **2015**, *34*, 1080–1084. [[CrossRef](#)]
36. United Nations Scientific Committee on the Effects of Atomic Radiation (UNSCEAR). *Sources and Effects of Ionizing Radiation: Sources*; United Nations Publications: New York, NY, USA, 2000.
37. Calusz-Moszek, J.; Białecka, B. Analysis of the possibilities of rare earth elements obtaining from coal and fly ash. *Gospod. Surowcami Miner. MRM* **2013**, *29*, 67–80.
38. Żelazny, S.; Świnder, H.; Jarośniński, A.; Białecka, B. The recovery of rare-earth elements from fly ash using alkali pre-treatment with sodium hydroxide. *Gospod. Surowcami Miner. MRM* **2020**, *36*, 127–144.
39. Ramakrishna, C.; Thenepalli, T.; Nam, S.Y.; Kim, C.; Ahn, J.W. The brief review on coal origin and distribution of rare earth elements in various coal ash samples. *J. Energy Eng.* **2018**, *27*, 61–69.

40. Zou, J.; Cheng, L.; Guo, Y.; Wang, Z.; Tian, H.; Li, T. Mineralogical and Geochemical Characteristics of Lithium and Rare Earth Elements in High-Sulfur Coal from the Donggou Mine, Chongqing, Southwestern China. *Minerals* **2020**, *10*, 627. [[CrossRef](#)]
41. Dai, S.; Zhao, L.; Hower, M.N.; Johnston, W.; Song, W.; Wang, P.; Zhang, S. Petrology, mineralogy and chemistry of size-fractionated fly ash from the Jungar power plant, Inner Mongolia, China, with emphasis on the distribution of rare earth elements. *Energy Fuels* **2014**, *28*, 1502–1514. [[CrossRef](#)]
42. Mastro, R.E.; Ram, L.C.; George, J.; Vetrivel, A.; Selvi, A.K.; Sinha, S.K.; Verma, T.K.; Rout, P.; Prabal, P. Impacts of opencast coal mine and mine fire on the trace elements' content of the surrounding soil vis-a-vis human health risk. *Toxicol. Env. Chem.* **2011**, *93*, 223–237. [[CrossRef](#)]
43. Kokowska-Pawłowska, M. Pierwiastki ziem rzadkich (REE) w iłowcach z wybranych pokładów węgla kamiennego serii mułowcowej i piaskowcowej Górnośląskiego Zagłębia Węglowego. *Gospod. Surowcami Miner. MRM* **2016**, *32*, 39–66. [[CrossRef](#)]
44. Nowak, J.; Kokowska-Pawłowska, M. Zmiany koncentracji wybranych pierwiastków ziem rzadkich (REEs) w odpadach węglowych (Changes in the concentration of some rare earth elements in coal waste). *Arch. Min. Sci.* **2017**, *62*, 495–507.
45. Migaszewski, Z.; Gałuszka, A. Pierwiastki ziem rzadkich w kwaśnych wodach kopalnianych—zarys problematyki. *Przegląd Geol.* **2019**, *67*, 105–114. [[CrossRef](#)]
46. Grawunder, A.; Merten, D.; Büchel, G. Origin of middle rare earth element enrichment in acid mine drainage-impacted areas. *Environ. Sci. Pollut. Res.* **2014**, *21*, 6812–6823. [[CrossRef](#)]
47. Dai, S.; Graham, I.T.; Ward, C.R. A review of anomalous rare earth elements and yttrium in coal. *Int. J. Coal Geol.* **2016**, *159*, 82–95. [[CrossRef](#)]
48. Nádudvari, Á.; Abramowicz, A.; Fabiańska, M.; Misz-Kennan, M.; Ciesielczuk, J. Classification of fires in coal waste dumps based on Landsat, Aster thermal bands and thermal camera in Polish and Ukrainian mining regions. *Int. J. Coal Sci. Technol.* **2020**, *1*, 1–16. [[CrossRef](#)]
49. Chang, C.; Li, F.; Liu, C.; Gao, J.; Tong, H.; Chen, M. Fractionation characteristics of rare earth elements (REEs) linked with secondary Fe, Mn, and Al minerals in soils. *Acta Geochim.* **2016**, *35*, 329–339. [[CrossRef](#)]
50. Lefticariu, L.; Klitzing, K.L.; Kolker, A. Rare Earth Elements and Yttrium (REY) in coal mine drainage from the Illinois Basin, USA. *Int. J. Coal Geol.* **2020**, *217*, 103327. [[CrossRef](#)]
51. Dai, S.; Jiang, Y.; Ward, C.R.; Gu, L.; Seredin, V.V.; Liu, H.; Zhou, D.; Wang, X.; Sun, Y.; Zou, J.; et al. Mineralogical and geochemical compositions of the coal in the Guanbanwusu Mine, Inner Mongolia, China: Further evidence for the existence of an Al (Ga and REE) ore deposit in the Jungar Coalfield. *Int. J. Coal Geol.* **2012**, *98*, 10–40. [[CrossRef](#)]
52. Hower, J.C.; Qian, D.; Briot, N.J.; Santillan-Jimenez, E.; Hood, M.M.; Taggart, R.K.; Hsu-Kim, H. Nano-Scale Rare Earth Distribution in Fly Ash Derived from the Combustion of the Fire Clay Coal, Kentucky. *Minerals* **2019**, *9*, 206. [[CrossRef](#)]
53. Hower, J.C.; Groppo, J.G.; Joshi, P.; Preda, D.V.; Gamliel, D.P.; Mohler, D.T.; Wiseman, J.D.; Hopps, S.D.; Morgan, T.D.; Beers, T.; et al. Distribution of Lanthanides, Yttrium, and Scandium in the Pilot-Scale Beneficiation of Fly Ashes Derived from Eastern Kentucky Coals. *Minerals* **2020**, *10*, 105. [[CrossRef](#)]
54. Pluta, I.; Pindel, T.; Janeczek, J. Aktywność izotopów radu w wodach kopalń Górnośląskiego Zagłębia Węglowego. *Wiad. Gor.* **2012**, *6*, 351–357.